5763: Roginolisib stabilizes inactive PI3Kδ to deliver specific target blockade with reduced immune toxicity

Oscar Vadas[1], Simon Tiede[2], Elise Solli[3,4], Maria Chaouki[5], Laura Tesmer[2], Shanlin Rao[2], Rémy Visentin[1], Mathias Wenes[6,7], Denis Migliorini[6,7], Sigrid S Skånland[3,4], Anne Quillet-Mary[5], Loïc Ysebaert[5], Julie Guillermet-Guibert[5], Alessio Bevilacqua[8], Lars van der Veen[9], Michael Lahn[8], Giusy Di Conza[8] Kjetil Taskén[3,4], Gerhard Hummer[2]

1 University of Geneva Protein Biochemistry Platform, Geneva, Switzerland, 2 Max Planck Institute for Biophysics, Frankfurt am Main, Germany, 3 Department of Cancer Immunology, Institute for Cancer Research, Oslo University Hospital, Norway, 4 KG Jebsen Centre for B-cell Malignancies, Institute of Clinical Medicine, University of Oslo, Norway,,5 Centre de Recherches en Cancérologie de Toulouse, Inserm, CNRS, Université de Toulouse, Labex Toucan, Toulouse, France, 6 Faculty of Medicine, University of Geneva, Switzerland, 7 Center for Translational Research in Onco-Hematology, University of Geneva, Switzerland, 8 iOnctura SA, Geneva, Switzerland, 9 iOnctura BV, Amsterdam, the Netherlands

Abstract

Introduction: Phosphoinositide 3-kinase (PI3K) is a key target in cancer therapy, but first-generation PI3K inhibitors were associated with toxicities limiting their clinical use. Roginolisib, a next-generation PI3Kδ inhibitor, is currently being investigated across multiple cancer types. In contrast to previous PI3K inhibitors, roginolisib has shown a well-tolerated profile. We hypothesize that this improved safety is in part due to roginolisib's high selectivity, driven by its structural properties.

Results: Structural and biophysical analyses—including X-ray crystallography, molecular dynamics simulations, and hydrogen-deuterium exchange mass spectrometry—demonstrate that roginolisib, unlike the first-generation inhibitor idelalisib, stabilizes the catalytic C-terminal helix (kα12) of PI3Kδ. This stabilization is specific for PI3Kδ and locks the enzyme in an inactive conformation, resulting in potent and sustained inhibition of PI3Kδ activity.

This inhibition profile is observed in tumor samples from patients with chronic lymphocytic leukemia (CLL) and in lymphoma cell lines. Although roginolisib and idelalisib exhibit similar potency in CLL cells, their effects on immune cells differ. Notably, high concentrations of idelalisib impair the cytotoxic activity of $CD8^+$ T cells and promote the differentiation of $CD4^+$ T cells towards Th17 and Th2 subsets. By contrast, roginolisib preserves $CD8^+$ T-cell function and does not alter CD4+ T-cell differentiation.

Conclusion: The mechanism of inhibition, herein described, likely based on conformational stabilization of the inactive kinase, is novel for PI3K small-molecule inhibitors. Hence, our findings may enable the development of a new generation of more efficacious and safer PI3K inhibitors.

1. Background

Cartoon depicting dormant and active state of PI3Kδ

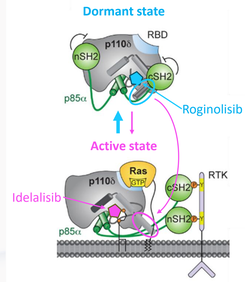

Adapted from Siempelkamp et al., 2017

All kinases, including PI3Kδ, exist in two major conformations, an active state with maximal enzyme activity and an inactive state with minimal enzyme activity, and utilize ATP to drive downstream signaling.

In inactive PI3Kδ, the C-terminal kα12 helix folds over the catalytic domain, to impede access to the active site.

Activation requires a conformational change where the C-terminus, specifically kα12, repositions away from the catalytic loop, allowing for membrane interaction and substrate binding.

Upon activation, the kα12 helix reorients from an "IN" to "OUT" conformation, allowing for the extension of the activation loop

Burke et al., Structure 2011
Vadas et al., Science signaling 2011

2. Molecular dynamics simulations show that roginolisib reorients C-terminal helix kα12 towards an inactive conformation

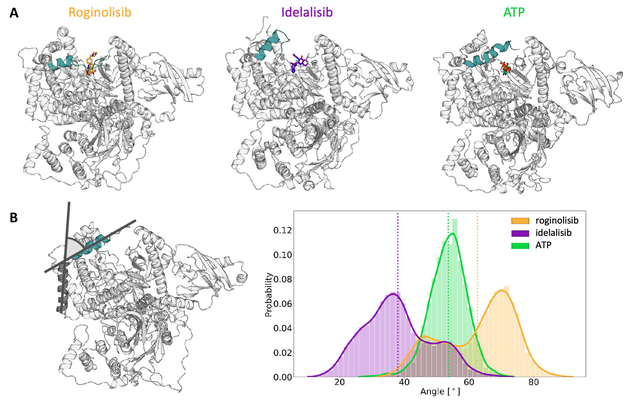

Difference in angle between PI3Kδ helix kα11 and the C-terminal helix kα12 in the presence of alternative bound ligands. **A** Representative simulation snapshots of roginolisib- (orange), idelalisib- (purple) and ATP- (green) bound structures with the C-terminal kα12 helix highlighted in teal. **B** Probability distribution of the angle formed between helix kα11 (grey) and kα12 (teal) across five replicates. The dotted lines represent the mean angle, corresponding to (62 ± 12) in the presence of roginolisib, (38 ± 11) with idelalisib and (54 ± 6) with ATP.

3. HDX/MS analysis of heterodimeric p110δ/p85α reveals how roginolisib limits kα12 conformational dynamics to stabilize the inactive enzyme and block its activation

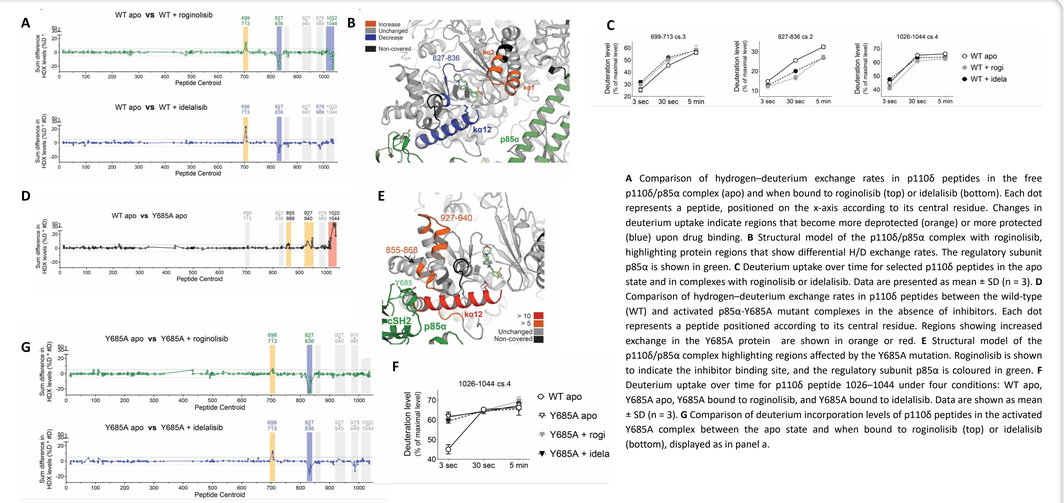

A Comparison of hydrogen–deuterium exchange rates in p110δ peptides in the free p110δ/p85α complex (apo) and when bound to roginolisib (top) or idelalisib (bottom). Each dot represents a peptide, positioned on the x-axis according to its central residue. Changes in deuterium uptake indicate regions that become more deprotected (orange) or more protected (blue) upon drug binding. **B** Structural model of the p110δ/p85α complex with roginolisib, highlighting protein regions that show differential H/D exchange rates. The regulatory subunit p85α is shown in green. **C** Deuterium uptake over time for selected p110δ peptides in the apo state and in complexes with roginolisib or idelalisib. Data are presented as mean ± SD (n = 3). **D** Comparison of hydrogen–deuterium exchange rates in p110δ peptides between the wild-type (WT) and activated p85α-Y685A mutant complexes in the absence of inhibitors. Each dot represents a peptide positioned according to its central residue. Regions showing increased exchange in the Y685A protein are shown in orange or red. **E** Structural model of the p110δ/p85α complex highlighting regions affected by the Y685A mutation. Roginolisib is shown to indicate the inhibitor binding site, and the regulatory subunit p85α is coloured in green. **F** Deuterium uptake over time for p110δ peptide 1026–1044 under four conditions: WT apo, Y685A apo, Y685A bound to roginolisib, and Y685A bound to idelalisib. Data are shown as mean ± SD (n = 3). **G** Comparison of deuterium incorporation levels of p110δ peptides in the activated Y685A complex between the apo state and when bound to roginolisib (top) or idelalisib (bottom), displayed as in panel a.

4. Roginolisib and idelalisib similarly inhibit PI3K signalling and reduce viability of chronic lymphocytic leukemia (CLL) B cells

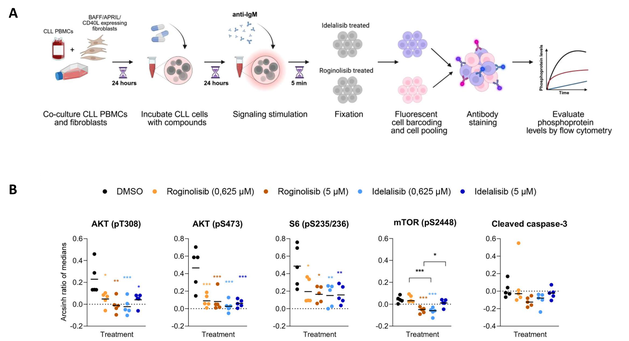

Roginolisib and idelalisib inhibit PI3K signaling and reduce viability of CLL B cells. **A** Phosphoflow workflow. PBMCs from CLL patients were co-cultured for 24 h with fibroblasts expressing BAFF, APRIL, or CD40L to prevent spontaneous apoptosis, then separated and treated with DMSO (0.1%), idelalisib, or roginolisib for 24 h. BCR signaling was induced with anti-IgM, and cells were fixed after 5 min. Samples were fluorescently barcoded, pooled, permeabilized, stained for phospho-proteins and CD19, and analyzed by flow cytometry. **B** CD19⁺ B cells were gated from PBMCs, and phospho-epitope levels are shown as arcsinh ratios normalized to unstimulated cells (set to 0; n = 5). Statistical analysis: two-way ANOVA with multiple-comparison correction ($P < 0.05$, $P < 0.01$, $P < 0.001$); non-significant comparisons not shown.

Solli et al., Molecular Oncology 2026

6. Unlike idelalisib, roginolisib preserves CD8 T-cell proliferation and effector function and does not influence CD4 T-cell differentiation

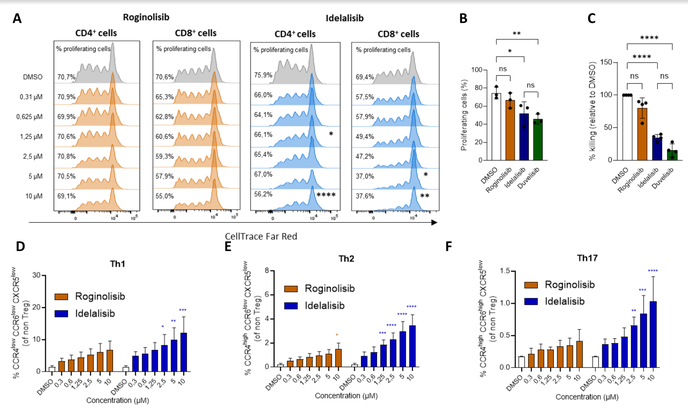

A CD3+ T cells were stained with CellTrace CFSE dye to assess proliferation, and next stimulated with anti-CD3/2/28-coated and treated with DMSO (0.1%) or indicated concentrations of roginolisib or idelalisib for 5 days, before proliferation was assessed by flow cytometry. The percentage of proliferating cells is indicated for each condition. The figure shows representative flow cytometry plots from n = 3 donors. **B** Aggregated proliferation data for roginolisib, idelalisib, and duvelisib (5 µM; mean ± SD, n = 3). **C** $CD8^+$ T cells from healthy donors were stimulated and treated with DMSO or 5 µM roginolisib, idelalisib, or duvelisib for 7 days, then co-cultured with calcein-labeled P815 cells for 4 h. Calcein release was used to quantify target cell death (mean ± SD, n = 3). **D-F** $CD4^+$ T cells from healthy donors were isolated, activated with anti-CD3/CD28, and treated for 48 h with idelalisib, roginolisib, or DMSO. **D** Frequency of $CCR4^{hi}CCR6^{low}CXCR5^{low}$ Th1 cells among non-Tregs ($CD4^+CD25^{low}$). **E** Frequency of $CCR4^{high}CCR6^{low}CXCR5^{low}$ Th2 cells among non-Tregs. **F** Frequency of $CCR4^{high}CCR6^{high}CXCR5^{low}$ Th17 cells among non-Tregs. Frequencies were determined by flow cytometry.
Statistical analysis: two-way ANOVA with multiple-comparison correction ($p < 0.05$, $p < 0.01$, $p < 0.001$); non-significant comparisons not shown.

Solli et al., Molecular Oncology 2026

Conclusion

Roginolisib uniquely stabilises the inactive state of PI3Kd by forcing a distinct configuration of the kα12 helix, keeping it in a closed position that prevents substrate interaction and activation.

This binding mode results in more sustained inhibition of phosphatidylinositol 3,4,5-trisphosphate (PIP3) formation in tumor samples of CLL patients.

Although inhibitory potency on malignant cells is maintained, selective engagement of the inactive kinase conformation appears to spare physiological immune-cell activation.

These molecular and cellular properties collectively translate into an improved clinical safety profile.

To date, PI3K inhibition through conformational stabilization of the inactive state has not been described. This mechanism may enable the development of a new generation of more selective, efficacious, and safer pharmacological strategies.

5. Roginolisib leads to an efficient PIP3 decrease in double–refractory CLL patient cells

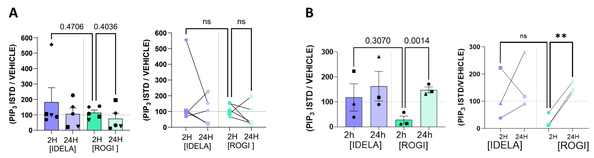

CTCs were isolated from CLL patient either **A** naïve of treatment or **B** double refractory and treated with vehicle, idelalisib (0.5µM) or roginolisib (0.5µM) followed by lipid extraction using chloroform/methanol solvent, addition of internal standards (ISTD) for normalization, and derivatization with TMS-diazo-methane to enhance detection sensitivity. Data are presented as % of VEHICLE at each time point. Each symbol represents a patient, to analyse time course evolution of each of them. A, C, E, Mean ± SEM. B,D,F Evolution of PIP3 level in each patient. ANOVA one-way test; *, p<0.05. All statistically different p-values are shown.

7. In the clinic, roginolisib shows differentiated safety profile compared to 1st generation PI3Kδ Inhibitors

All causality Adverse Events	Roginolisib FiH 80 mg Dose	Idelalisib	Copanlisib	Duvelisib	Umbralisib
	N = 28	N = 146	N = 244	N = 442	N = 371
Median exposure, months (Range)	5.6 0.9, 65.5	6.1 0.3, 26.4	4.3 0.2, 47.4	9.0 0.1, 53	5.9 0.1, 75.1
Actions due to AE					
Discontinuation	3%	23%	24%	35%	15%
Dose reduction	3%	41%	24%	23%	10%
Toxicity					
SAE	14%	50%	51%	65%	26%
Death due to AE	3%	8%	5%	4%	NR
Grade ≥3 AE	34%	71%	85%	84%	51%
Grade ≥3 AEs					
Grade ≥3 Infection	0%	23%	23%	27%	20%
Grade ≥3 Neutropenia[a]	2%	28%	29%	43%	17%
Grade ≥3 Diarrhea or Colitis	3%	14%	5%	23%	7%
Grade ≥3 AST/ALT increase[a]	10%	18%	2%	8%	7%
Grade ≥3 Rash	0%	4%	2%	9%	3%
Any Grade Pneumonitis	0%	5%	7%	7%	1%
Grade ≥3 Hyperglycaemia[a]	0%	0%	34%	0%	0%
Grade ≥3 Hypertension	3%	0%	29%	0%	0%

Comparative table outlining the safety outcomes of roginolisib from preliminary Phase I study versus other PI3Kδ inhibitors.

Source: FDA ODAC 2022 (Table 9); iOnctura, Di Giacomo et al., under review
FiH, First-in Human; NR, not reported.

[a] Incidence based on laboratory data
[b] Data cut off 6 Jan 26 (80 mg rogi)